Steel and Composite Structures, *Vol. 23, No. 4 (2017) 445-452*
DOI: https://doi.org/10.12989/scs.2017.23.4.445

Numerical study of internally reinforced circular CFT column-to-foundation connection according to design variables

Hee-Ju Kim [1a], Junsu Ham [2b], Ki-Tae Park [3c] and Won-Sup Hwang [*2]

[1] *Construction R&D Department, Korea Agency for infrastructure Technology Advancement, 286 simin-Daero, Dongan, Anyang-si, Gyeonggi, 14066, Korea*
[2] *Department of Civil Engineering, Inha University, 100 Inha-ro, Nam-gu, Incheon 22212, Republic of Korea*
[3] *Structural Engineering Research Institute, Korea Institute of Civil Engineering and Building Technology, 283 Goyangde-ro, Ilsanseo-gu, Goyang-si, Gyeonggi-do, 10223 Republic of Korea*

(*Received January 21, 2016, Revised December 16, 2016, Accepted January 18, 2017*)

Abstract. This study intends to improve the structural details of the anchors in the conventional CFT column-to-foundation connection. To that goal, finite element analysis is conducted with various design variables (number and embedded length of deformed bars, number, aspect ratio, height ratio and thickness ratio of ribs) selected based upon the results of loading test and strength evaluation. The finite element analysis is performed using ABAQUS and the analytical results are validated by comparison with the load-displacement curves obtained through loading test applying axial and transverse loads. The behavioral characteristics of the numerical model according to the selected design variables are verified and the corresponding results are evaluated.

Keywords: CFT column-to-foundation; finite element analysis; anchors; deformed bars; ribs

1. Introduction

The column-to-foundation connection transfers the large compression forces developed in the structure to the foundation. Since this connection is located at the bottom of the structure, it is the part concentrating most of the stresses generated by diverse loads and is thus the most important part of the structure in terms of the structural strength. This column-foundation connection must be designed to develop sufficient strength against the load combination involving the vertical load produced by the weight of the structure and the live loads caused by wind and earthquake. The usage of anchors in the connection becomes more frequent considering the functions and constructability of such structure. Therefore, an anchor frame is installed in concrete to let sufficient strength to develop during the erection of the column-foundation connection and results in the enlargement of the foundation.

The type of column-foundation connection currently applied in the design is depicted in Fig.1 together with its structural details. The connection is realized using anchors. In the design, the concrete at the bottom of the base plate installed in the connection resists to the compressive forces whereas the anchor bolts and anchor frame resist to the tensile forces. The horizontal forces are assumed to be sustained by the anchor bolts and the corresponding shear forces are assumed to be uniformly distributed in the anchor bolts. Ribs are installed between the upper and lower base plates. In addition, the anchor frame is fabricated with complicated interconnection of the steels inside concrete. Such situation results in the enlargement of the foundation and in complicated and conservative design leading to the loss of economic efficiency.

In order to solve these problems, Kim *et al*. (2015) simplified the structural details and improved the constructability of the column-foundation connection by adopting high-tension bolts instead of the common anchors. These authors also enhanced the performance of the connection by increasing the stiffness using internal reinforcing bars and conducted tests to verify the performance. The experimental results enabled to validate the applicability of a new type of connection using high-tension bolts and internal rebar improving the structural details of the circular steel column-foundation connection.

This study intends to derive the optimal shape of the structural details applying high-tension bolts by means of numerical analysis considering various design variables. The ribs located in the base connect the upper and lower base plates and transfer the loads to the foundation (Dessouki *et al*. 2014). The ribs are thus critical members that must be considered as design variable. Therefore, the design variables are chosen to be the structural details of the ribs in the steel column-foundation connection with double base plate together with the number and embedded length of the deformed bars proposed as internal reinforcement. The effect of these design variables is evaluated by numerical analysis.

*Corresponding author, Professor,
E-mail: hws@inha.ac.kr
[a] Ph.D., E-mail: heeju@kict.re.kr
[b] Ph.D. Student, E-mail: nuljoahe@gmail.com
[c] Ph.D., E-mail: ktpark@kict.re.kr

ISSN: 1229-9367 (Print), 1598-6233 (Online)

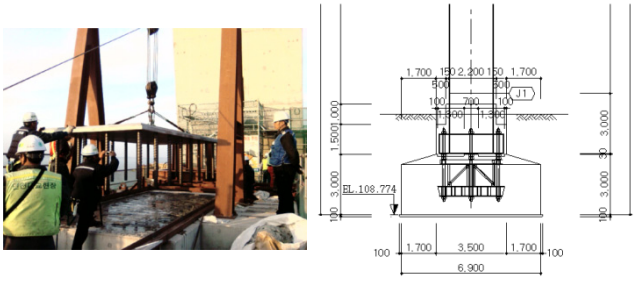

Fig. 1 Erection of column-to-foundation connection and structural details

2. Modeling and analysis method of CFT column-foundation connection

2.1 Detailed dimensions of numerical model

The specimen selected for the numerical analysis model is the steel column-foundation specimen with insertion of deformed bars among the specimens proposed by Kim *et al*. (2015). This specimen presents simplified structural details by removing the anchor frame traditionally installed in previous foundation concrete and by using high strength anchors. And then, in the experiment, an axial and transverse load is simultaneously applied to the specimen to investigate behavior of the proposed column-foundation connection.

As shown in Fig. 2, the specimen uses 8 high-tension bolts and a double base plate to connect the steel column and the foundation. In addition, 16 bars are installed inside the column to improve the performance of the connection between the column and the foundation. The total length of the column (l) is 2,500 mm. The steel tube presents an outer diameter (D) of 518 mm and an inner diameter (D_i) of 500 mm. The column is a CFT (Concrete Filled Tube). The base plates with thickness of 25 mm are disposed at the bottom of the column with spacing of 375 mm. The upper and lowr base plates are connected by 15 mm thick ribs. The dimensions of the foundation concrete are 2210×1710×900 mm (L×H×B). The dimensions of the model are listed in Table 1.

Table 1 Dimensions of numerical model

Part			Dimensions
Column	Length of shaft (l, mm)		2,500
	Diameter (mm)	Outer (D)	518
		Inner (D_i)	500
Base	Spacing of base plate (D_b, mm)		375
	Thickness of base plate (t_b, mm)		25
	Thickness of rib (t_r, mm)		15
Foundation	Width (L, mm)		2,210
	Depth (H, mm)		1,710
	Height (B, mm)		900

2.2 Material properties

For the finite element analysis of the internally reinforced column-foundation connection, the definitions of the steel and concrete materials can be expressed as follows. The stress-strain relation of the steel used for the steel tube and the base adopts the formula suggested by Nishimura (1997) as shown in Fig. 3 and Eq. (1), and the material

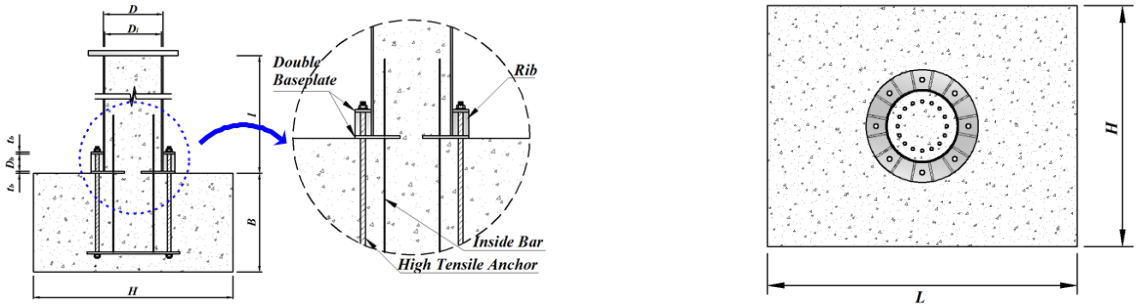

Fig. 2 Structural details and dimensions of column-to-foundation connection

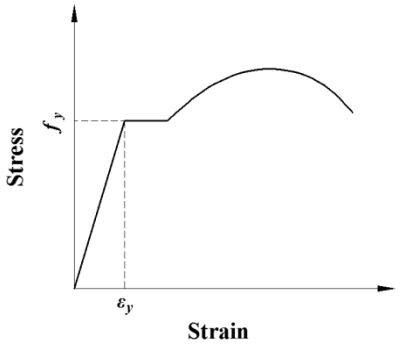

Fig. 3 Stress-strain relation of steel

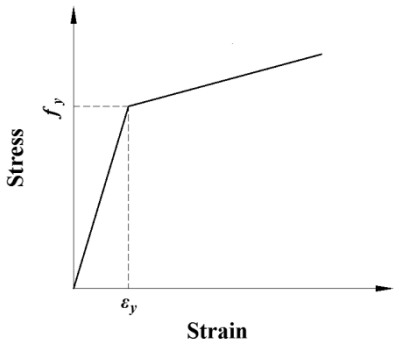

Fig. 4 Stress-strain relation of high-tension bolt and reinforced bar

Table 2 Material properties for steel

Material	Steel grade	E (MPa)	f_y (MPa)	E_{st}^P (MPa)	ε_{st}^P	a	b
Steel	SM490	20,500	323	5430	0.0185	3440	0.0484

Table 3 Material properties for high-tension bolt and reinforced bar

Material	Steel grade	Elastic modulus (E, MPa)	Tangent modulus (E_t, MPa)	Yield strength (f_y, MPa)
High-tension bolt	F8T	20,500	$\frac{E}{100}$	695
Reinforced bar	SD400			433

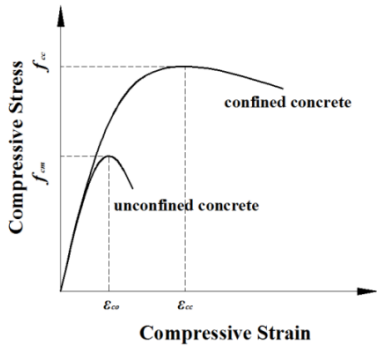

Fig. 5 Stress-strain relation of concrete

properties are arranged in Table 2 of which values were obtained by material test. SM490 is adopted for the steel tube and the ribs. The steel grade and diameter of the high-tension bolts and rebar are F8T and 30 mm, and SD400 and 22 mm. For the high-tension bolt and the rebar, bi-linear relation is applied as shown in Fig. 4. Also, the stress-strain relation of the concrete used in this study adopts the formula proposed by Park *et al*. (2012) as shown in Fig. 5. The concrete inside the steel tube applies the constitutive equations of concrete considering the confining effect of the steel tube. The foundation concrete applies the constitutive equations of the non-confined concrete.

$$f = a \cdot \ln\left(\frac{\varepsilon_{mon}^P}{b} + 1\right) + \left(E_{st}^P - \frac{a}{b}\right) \cdot \varepsilon_{mon}^P + f_y \quad (1)$$

where, ε_{mon}^P : Plastic strain with the point of strain hardening (ε_{st}^P) as the origin

E_{st}^P : Strain hardening gradient (MPa)

f_y : Yield strength (MPa)

a, b : Material constants

2.3 Modeling and analysis method

Fig. 6 presents the discretization of the numerical model for the specimen with reinforced internal rebar. The commercial finite element analysis program ABAQUS 6.10 was used to examine the behavioral characteristics of each design variable.

Steel and concrete were modeled as eight-noded brick solid elements of Type C3D8 (Su 2004, Lee and Goel 2008, Hu *et al*. 2010, Drosopoulos *et al*. 2012, Ashakul and Khampa 2014, Liu *et al*. 2014). However, this resulted in a complicated process when applying the same elements for the high-tension bolt and the internal rebar and in tremendously difficult node-sharing between elements, which were likely to degrade the accuracy of the analysis

Table 4 Material properties for concrete

Material	Elastic modulus (E, MPa)	Compressive strength (f_c, MPa)
Confined concrete	25,978	28
Foundation concrete	27,996	40

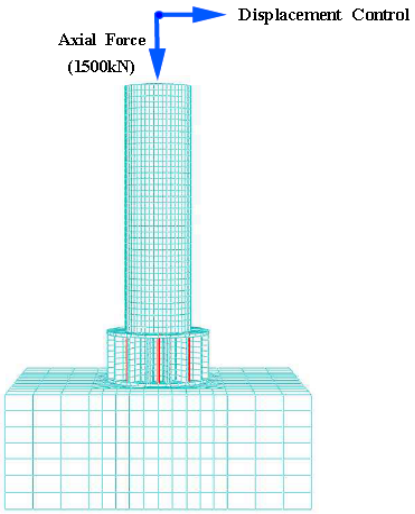

Fig. 6 Numerical model if internally reinforced column-to-foundation connection

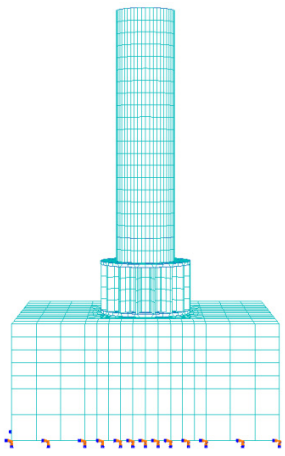

Fig. 7 Boundary conditions applied in column-to-foundation connection model

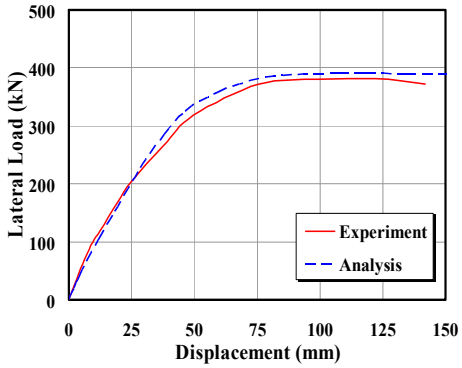

Fig. 8 Comparison of experimental and analytical load-displacement curves

and increase the computational efforts. This problem was solved by modeling the high-tension bolt and the internal rebar by beam elements to connect the foundation concrete and the base plates. Moreover, the embedded function was applied to the beam elements modeling the high-tension bolt and the internal rebar to reproduce the bond force with concrete (Lee *et al*. 2011, Hwang *et al*. 2013).

In order to consider the effect of the contact surface of each element, coefficients of friction were applied to the contact surface between the steel tube and the confined concrete and the contact surface between the base plate and the foundation concrete (Hu *et al*. 2010, Shiming and Huifeng 2012). In addition, the welds of the base plates, ribs and steel tube were assumed as perfectly bonded for the analysis. The nodes were shared between the elements to minimize the error in the analysis. The boundary conditions and load conditions of the numerical model are shown in Fig. 7. The displacement and rotation are restrained at the bottom of the foundation, anchor bolts and rebar to apply loads identical to the test. An axial load of 1,500 kN is applied and the horizontal load is applied by displacement control.

2.4 Validity check of numerical model

The validity of the numerical model proposed in this study is verified by comparing the experimental and analytical load-displacement curves of the internally reinforced specimen as shown in Fig. 8. The slopes of the experimental and analytical results exhibit similar trend in the early elastic region and there is also nearly no difference in the yield point of the structure. The maximum load of the internally reinforced connection is 381.64 kN and the analysis gives a value of 386.47 kN, which represents an error of about 1%. These results indicate that the analysis method proposed in this study simulates accurately the behavior of the actual structure. Accordingly, the investigation of the various design variables can be conducted using the proposed analysis method.

3. Behavioral characteristics per design variable for deformed rebar

In the circular CFT column-foundation connection, the steel column and the foundation concrete are connected by high-tension bolts installed externally. The internal bars are installed inside to increase the stiffness of the connection. In view of such structure, different behavioral characteristics are likely to occur according to the number of internal bars and according to the embedded length of the bars from the foundation concrete to the steel column. Therefore, the internal bar is chosen as design variable and numerical analysis is performed with regard to the number of bars (BA-series) and the embedded length of the bar inside the

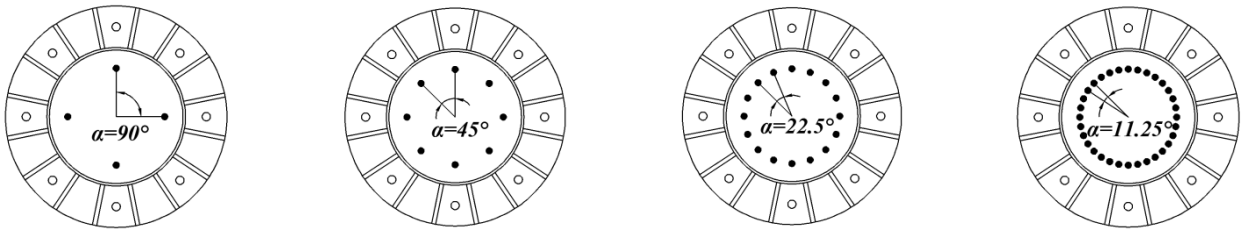

(a) BA-90 (b) BA-45 (c) BA-22.5 (d) BA-11.25

Fig. 9 Shape of BA-series

Table 5 Variables of numerical models of internal bars

Model		NO., n	α (degree)	$\frac{n}{n_a}$	Model		L_b (mm)	$\frac{L_b}{D_c}$
BA-series	BA-90	4	90	0.5	BL-series	BL-0.25	125	0.25
	BA-45	8	45	1.0		BL-0.5	250	0.5
	BA-22.5	16	22.5	2.0		BL-1.0	500	1.0
	BA-11.25	32	11.25	4.0		BL-1.25	625	1.25
						BL-1.5	750	1.5
						BL-2.0	1000	2.0

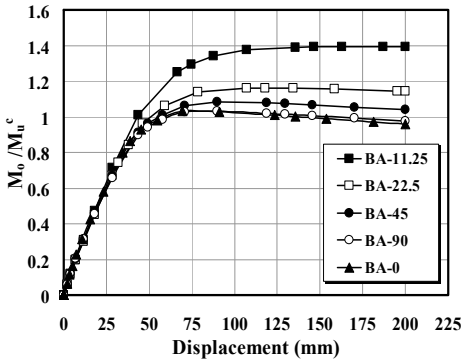

Fig. 10 Moment ratio-displacement curves of BA-series models

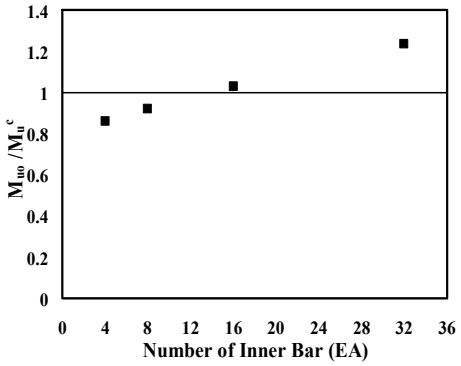

Fig. 11 Effect of number of internal bars on ultimate strength

column (BL-series) as shown in Table 5.

3.1 Effect of number of deformed bars

Fig. 10 compares the moment ratio-displacement curves of the BA-series models. Here, M_u^c is the ultimate strength of the column from the theoretical formula (Chung and Matsui 2005). The number of internal bars depends on their arrangement. As shown Fig. 9, the regular arrangements at central angles of 90°, 45°, 22.5° and 11.5° give respectively 4, 8, 16 and 32 bars (Table 5). For effect of number of deformed bars, the embedded length of the internal bar is 625 mm, 16 ribs are used, the rib shape ratio is 0 and the rib thickness is 15 mm.

Model BA-0 without internal rebar is examined additionally to compare the strength increase effect with respect to the reinforcement method of the internal bars. The strength increase according to the arrangement of the internal bars is larger as much as the number of internal bars arranged inside the structure is large and as much as the central angle of the internal bars arranged inside is small. This indicates that the arrangement of internal bars purposed for the improvement of the efficiency of the high-tension bolts used in the anchor part can be favorable for the increase of the strength. The largest strength increase is achieved by model BA-11.25 with 32 internal bars.

Fig. 11 plots the ratio of the analytical ultimate strength M_u^c according to the number of bars to examine the effect of the arrangement angle (α) of the internal bars. For the internally reinforced connection, the strength increase effect is larger as much as the number of internal reinforced bars is large. It appears that more than 16 internal bars (BA-45) shall be reinforced to achieve sufficient ultimate strength and that the strength increase proportionally according to the arrangement of bars for a number of bars larger than 16.

3.2 Effect of embedded length of deformed bars

Fig. 12 compares the moment ratio-displacement curves of the BL-series models. The embedded length of the internal bar means the anchored length measured longitudinally from the bottom of the column. This length can be expressed in terms of ratios by comparison with the diameter of steel and the location of deformed bars is in Fig. 9(c). In this case, 16 deformed bars and 16 ribs are used, the rib shape ratio is 0 and the rib thickness is 15 mm.

In Fig. 12, there is practically no difference in the ultimate strength between model BL-0.25 presenting the shortest embedded length of the internal bar and model BL-2.0 corresponding to a length of 1.000 mm. This indicates that the embedded length of the internal bar has very poor effect on the strength of the structure.

Fig. 13 plots the ratio of the analytical ultimate strength M_{u0} to the theoretical ultimate strength M_u^c with respect to the number of bars, and expresses the effect related to L_b/D_c, that is the ratio of the embedded length of the internal

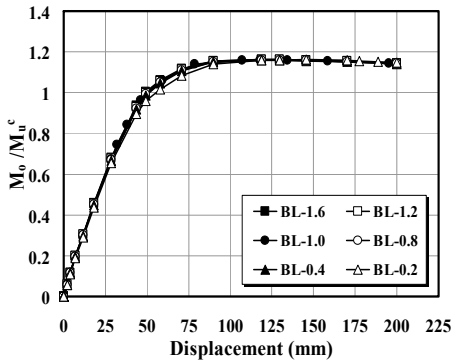

Fig. 12 Moment ratio-displacement curves of BL-series models

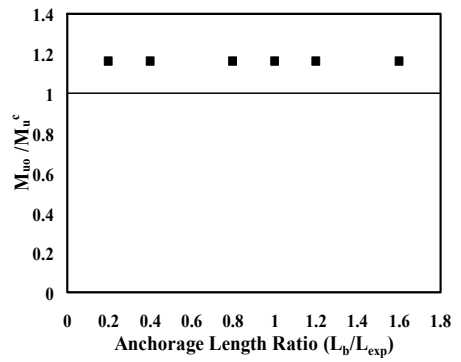

Fig. 13 Effect of embedded length ratio of internal bars on ultimate strength

Table 6 Dimensions of numerical models of ribs

Model		No., n	$\frac{n}{n_{exp}}$	Model		b_r (mm)	$\frac{b_r}{h_r}$	Model		t_r (mm)	$\frac{h_r}{t_r}$
RA-series	RA-90	4	0.25	RS-series	RS-0	0	0	RT-series	RT-75	5	75
	RA-45	8	0.5		RS-0.25	93.75	0.25		RT37.5	10	37.5
	RA-22.5	16	1.0		RS-0.5	187.5	0.5		RT-25	15	25
	RA-11.25	32	2.0		RS-0.75	281.25	0.75		RT-18.75	20	18.75
					RS-1.0	375	1.0		RT-15	25	15
									RT-12.5	30	12.5

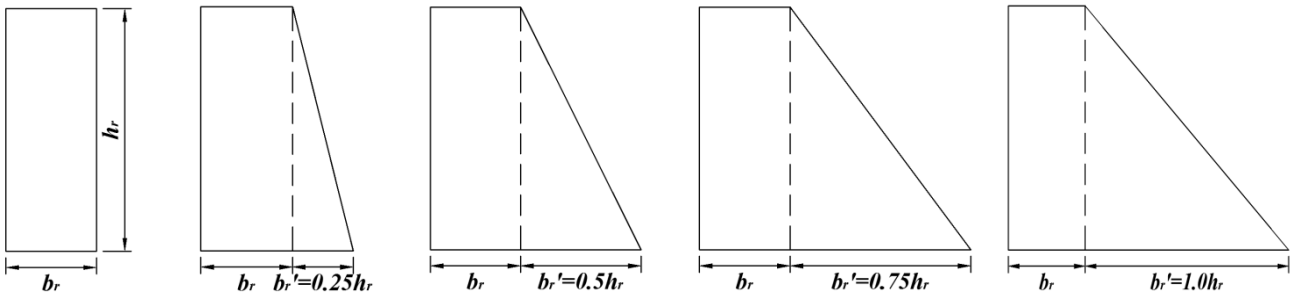

(a) RS-0 (b) RS-0.25 (c) RS-0.5 (d) RS-0.75 (e) RS-1.0

Fig. 14 Shape of RS-series

bar to the diameter of the steel tube. It appears that there is practically no strength increase effect related to the embedded length of the internal bar and the diameter of the steel tube. The strength relative to the internal bar seems to be more influenced by the number of bars than by the length of the bar.

4. Behavioral characteristics per design variable for rib

The ribs forming the double base plate supporting the high-tension bolts are important members transferring the loads to the foundation. Table 6 lists the design variables relative to these ribs for the numerical analysis. Analysis is performed for the ribs with respect to the number of internal bars (RA-series) according to the central angle (α) of the circular section, the aspect ratio of the ribs (RS-series), and the height-to thickness ratio of the ribs (RT-series).

4.1 Effect of number of ribs

Fig. 15 compares the moment ratio-displacement curves of the RA-series models. Since the number of installed ribs depends on their arrangement, the regular arrangement at central angles of 90°, 45°, 22.5° and 11.5° give respectively 4, 8, 16 and 32 ribs (Table 6). In order to investigate effect of the number of ribs, the number of internal bars is 16, the embedded length is 625 mm, the rib shape ratio is 0 and the rib thickness is 15 mm.

The strength increase effect according to the arrangement of ribs is seen to be larger as much as the number of ribs arranged in the base is large and as much as the central angle of the ribs arranged inside is small. Models RA-45 and RA-90 develop reduced strength compared to model RA-22.5. This indicates that ribs shall be disposed beyond a definite number to let the high-tension bolts develop their performance.

Fig. 16 plots the ratio of the analytical ultimate strength

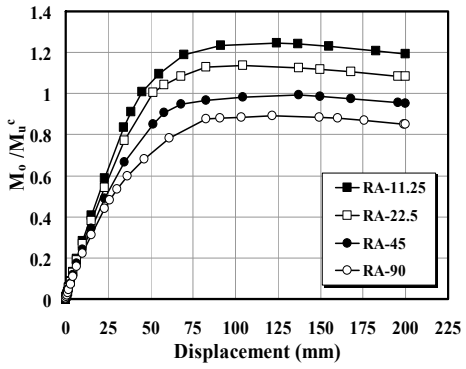

Fig. 15 Moment ratio-displacement curves of RA-series models

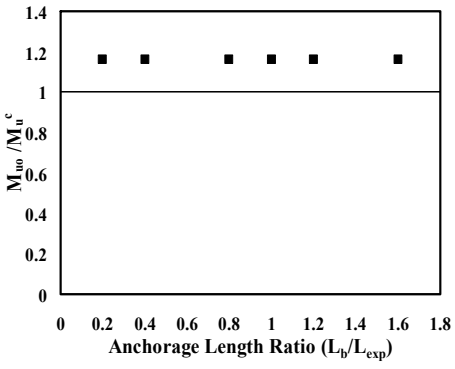

Fig. 16 Effect of number of ribs on ultimate strength

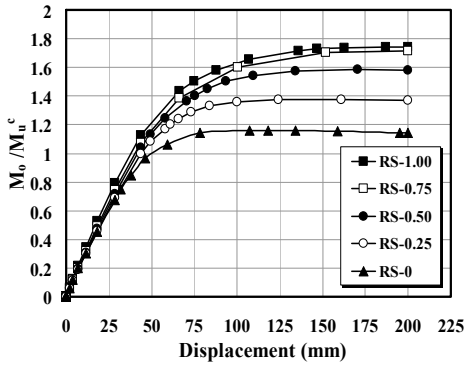

Fig. 17 Moment ratio-displacement curves of RS-series models

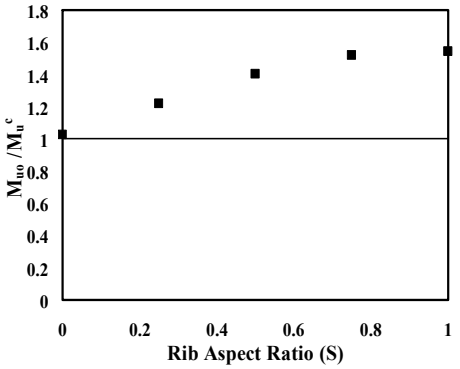

Fig. 18 Effect of aspect ratio of ribs on ultimate strength

M_{u0} to the theoretical ultimate strength M_u^c to examine the effect of the number of ribs located in the base. The strength reduces as much as the number of ribs is small in the structural details of the internally reinforced connection. It appears that a minimum of 16 ribs shall be installed to let the high-tension bolts develop their performance. However, since the central angle of the ribs is also correlated to the number of high-tension bolts arranged in the base, the number of ribs shall be determined considering the arrangement of the high-tension bolts.

4.2 Effect of rib shape

Fig. 17 compares the moment ratio-displacement curves of the RS-series models. The models of the RS-series are established with respect to the aspect ratio of the ribs ranging from 0.25 to 1.00, where the aspect ratio is defined as the ratio of the height (h_r) to the extended length (b_r') of the rib. For effect of rib shape, 16 bars are installed, embedded length is 625 mm, the number of ribs is 16, and the rib thickness is 15mm.

As shown in Fig. 14, the aspect ratio of the rib expresses the effect related to the size of the base plate located at the bottom of the plate. Unlike model RS-0 corresponding to the conventional rectangular shape of the rib, the modification of the shape of the rib to a trapezoid shape is seen to provide strength increase effect. However, the strength increase rate appears to reduce gradually for aspect ratios beyond that of RS-0.5 and to be practically zero beyond RS-0.75.

Fig. 18 presents the effect of the aspect ratio ($S = b_r' / h_r$) of the ribs on the dimensionless ultimate strength. Large size of the base plates located at the bottom of the base is seen to have favorable effect on the strength increase. Beside, no further increase of the strength occurs for aspect ratios higher than 0.75. An aspect ratio of 0.5 corresponding to approximately half of the rib height seems to be appropriate to provide proportional effect. In addition, even if large aspect of the rib can increase the strength, need is to consider the corresponding enlargement of the foundation. Accordingly, the aspect ratio of 0.75 appears to be the threshold beyond which the strength will not increase further in the case of the internally reinforced connection proposed in this study.

4.3 Effect of height-to-thickness ratio of rib

Fig. 19 compares the moment ratio-displacement curves of the RT-series models. The models of the RT-series are established with respect to the thickness ratio of the ribs ranging from 12.5 to 75.0, where the thickness ratio is defined as the ratio of the height (h_r) to the thickness (t_r) of the rib. For effect of height-to-thickness ratio of rib, the number of bars is 16, embedded length is 625 mm, the number of ribs is 16, and the rib shape ratio is 0.

Recalling that the rib plays the role of stiffener for the

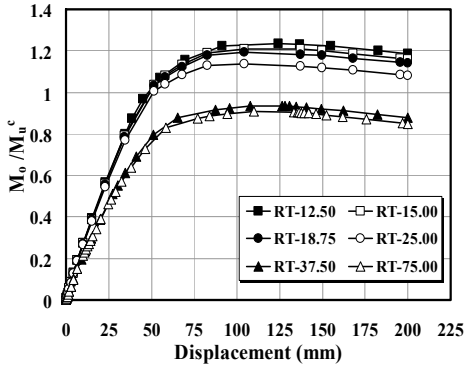

Fig. 19 Moment ratio-displacement curves of RT-series models

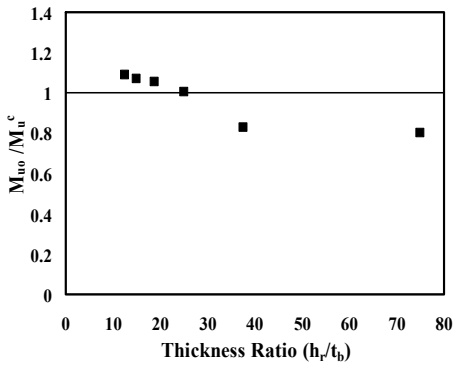

Fig. 20 Effect of thickness ratio of ribs on ultimate strength

double base plate, it appears that the strength increase effect degrades when the height-to-thickness ratio of the rib becomes larger than 37.5 (10 mm). When the thickness of the ribs is thin, the strength reduces due to the loss of stiffness in the connection to transfer the loads acting on the column to the foundation concrete and anchors. In such case, the strength increase effect can be achieved by securing a minimum height-to-thickness ratio of 25 corresponding to a rib thickness of 15mm.

Fig. 20 plots the ratio of analytical ultimate strength M_{u0} to the theoretical ultimate M_u^c with respect to the height-to-thickness ratio (h_r/t_r) of the ribs. The strength increase effect varies according to the thickness ratio of the ribs. For ratio smaller than 25 (15 mm), the high-tension bolts cannot develop their performance and the strength tends to decrease. For ratio larger than 25 (15 mm), the strength increases but by a small increment. Accordingly, the ribs arranged in the base shall secure a minimum ratio of 25 (thickness of 15 mm) to increase the strength of the connection.

5. Conclusions

This study conducted numerical analyses to evaluate the effect of selected design variables on the behavioral characteristics of the steel column-foundation connection subjected simultaneously to flexural moment and shear force. These design variables were the internal bars and the ribs playing the role of stiffener in the connection.

The following conclusions can be drawn from the study.

- Finite element analysis was performed with reference to the improved structural details of the internally reinforced column-to-foundation connection and the results were compared to the experimental data to validate the validity of the analysis method. The design variables of each of the internally reinforced connections were selected and the finite element analysis results were compared to the ultimate strength of the column.
- In the case of the reinforced internal bars, the effect of the number of bars was seen to be more decisive than the effect related to the embedded length of the bars installed in the column. The installation of minimum 16 internal bars appeared to be recommendable in terms of the strength.
- The analysis revealed that a minimum of 16 ribs should be secured to improve the performance of the high-tension bolts. Since the number of ribs is influenced by the arrangement or the number of high-tension bolts, the number of ribs shall be determined considering the arrangement of the high-tension bolts.
- No further increase of the strength occurred for aspect ratios of the rib higher than 0.75. For the structural details with reinforcement by internal bars, the appropriate number of ribs appeared to be 8 and a height-to-thickness ratio of the ribs larger than 25 (rib thickness of 15 mm) should be secured to let the structure develop its performance.

Acknowledgments

This work was supported by INHA UNIVERSITY Research Grant.

References

AISC (2011), Steel Construction Manual; American Institute of Steel Construction.

Ashakul, A. and Khampa, K. (2014), "Effect of plate properties on shear strength of bolt group in single plate connection", *Steel Compos. Struct., Int. J.*, **16**(6), 611-637.

Chung, J.A. and Matsui, C. (2005), "SRC standards in Japan and comparison of various standards for CFT columns", *Int. J. Steel Struct.*, **5**, 315-323.

Dessouki, A.K., Yousef, A.H. and Fawzy, M.M. (2014), "Stiffener configurations of beam to concrete-filled tube column connections", *Steel Compos. Struct., Int. J.*, **17**(1), 83-103.

Drosopoulos, G.A., Stavroulakis, G.E. and Abdalla, K.M. (2012), "3D Finite element analysis of end – plate steel joints", *Steel Compos. Struct., Int. J.*, **12**(2), 93-115.

Hu, H.T., Su, F.C. and Elchalakani, M. (2010), "Finite element analysis of CFT columns subjected to pure bending moment", *Steel Compos. Struct., Int. J.*, **10**(5), 415-428.

Hwang, W.S., Kim, H.J., Ham, J.S. and Hwang, S.H. (2013), "Study on rib's structural details of double baseplate connection through numerical analysis", *J. Korea Inst. Struct. Maint. Insp.*, **15**(2), 45-53. [In Korean]

Kim, H.J., Hu, J.W. and Hwang, W.S. (2015), "Cyclic testing for structural detail improvement of CFT column-foundation connections", *Sustainability*, **7**, 5260-5281.

Lee, D.Y. and Goel, S.C. (2008), "Exposed column-base plate connections bending about weak axis: 1. numerical parametric study", *Int. J. Steel Struct.*, **8**(1), 11-27.

Lee, H.L., Kim, H.J. and Hwang, W.S. (2011), "Behavior of the foundation of concrete filled steel tubular pier", *J. Comput. Struct. Eng. Inst. Korea.*, **24**(5), 491-498. [In Korean]

Liu, Y., Málaga-Chuquitaype, C. and Elghazouli, A.Y. (2014), "Behavior of open beam-to-tubular column angle connections under combined loading conditions", *Steel Compos. Struct., Int. J.*, **16**(2), 157-185.

Nishimura, N. (1997), "A study on improvement in the cyclic plasticity model and introduction of finite element method", Research Report, 07455185. [In Japanese]

Park, Y.M., Hwang, W.S., Yoon, T.Y. and Hwang, M.O. (2005), "A new base plate system using deformed reinforcing bars for concrete filled tubular column", *Steel Compos. Struct., Int. J.*, **5**(5), 375-394.

Park, K.D., Kim, H.J. and Hwang, W.S. (2012), "Experimental and numerical studies on the confined effect of steel composite circular columns subjected to axial load", *Int. J. Steel Struct.*, **12**(2), 253-265.

Shiming, C. and Huifeng, Z. (2012), "Numerical analysis of the axially loaded concrete filled steel tube columns with debonding separation ate the steel-concrete interface", *Steel Compos. Struct., Int. J.*, **13**(3), 277-293.

Su, F.C. (2004), "Numerical analysis of concrete filled tubes subjected to pure bending", M.S. Dissertation; Department of Civil Engineering, National Cheng Kung University, Tainan, Taiwan, R.O.C. [In Chinese]

CC